where the units of $\delta\theta$ are the same as those of θ_B. The relative error $(\delta\theta/\theta_B)$ is a function of E/N_0 only. The angular error can be many times less than the beamwidth, depending upon the value of E/N_0. The accuracy formulas derived previously for the time delay and the frequency may be readily applied to the determination of the angular error for various aperture distributions.

The effective aperture width γ for several aperture distributions which can be computed analytically are given below:

Parabolic distribution

$$A(x) = 1 - \frac{4(1-\Delta)x^2}{D^2} \qquad |x| < \frac{D}{2},\ \Delta < 1$$

$$\begin{aligned} &\text{For } \Delta = 0 && \gamma^2 = 0.863D^2 \\ &\text{For } \Delta = 0.5 && \gamma^2 = 1.88D^2 \\ &\text{For } \Delta = 1.0 && \gamma^2 = 3.287D^2 \end{aligned} \tag{11.43}$$

Cosine distribution

$$A(x) = \cos\frac{\pi x}{D} \qquad |x| < \frac{D}{2}$$

$$\gamma^2 = 1.286D^2 \tag{11.44}$$

Triangular distribution

$$A(x) = 1 - \frac{2}{D}|x| \qquad |x| < \frac{D}{2}$$

$$\gamma^2 = 0.986D^2 \tag{11.45}$$

Inverse probability, likelihood ratio, and accuracy. The method of inverse probability as described by Woodward[5] can be used as a basis for determining the theoretical accuracies associated with radar measurements. The likelihood function also can be used for deriving measurement accuracy.[9] Both methods result in accuracy expressions like that of Eq. (11.17).

11.4 AMBIGUITY DIAGRAM[5,10–12]

The ambiguity diagram represents the response of the matched filter to the signal for which it is matched as well as to doppler-frequency-shifted (mismatched) signals. Although it is seldom used as a basis for practical radar system design, it provides an indication of the limitations and utility of particular classes of radar waveforms, and gives the radar designer general guidelines for the selection of suitable waveforms for various applications.

The output of the matched filter was shown in Sec. 10.2 to be equal to the cross correlation between the received signal and the transmitted signal [Eq. (10.18)]. When the received echo signal from the target is large compared to noise, this may be written as

$$\text{Output of the matched filter} = \int_{-\infty}^{\infty} s_r(t)s^*(t - T_R')\,dt \tag{11.46}$$

where $s_r(t)$ is the received signal, $s(t)$ is the transmitted signal, $s^*(t)$ is its complex conjugate, and T_R' is the estimate of the time delay (considered a variable). Complex notation is assumed in Eq. (11.46). The transmitted signal expressed in complex form is $u(t)e^{j2\pi f_0 t}$, where $u(t)$ is the

complex-modulation function whose magnitude $|u(t)|$ is the envelope of the real signal, and f_0 is the carrier frequency. The received echo signal is assumed to be the same as the transmitted signal except for the time delay T_0 and a doppler frequency shift f_d. Thus

$$s_r(t) = u(t - T_0)e^{j2\pi(f_0 + f_d)(t - T_0)} \tag{11.47}$$

(The change of amplitude of the echo signal is ignored here.) With these definitions the output of the matched filter is

$$\text{Output} = \int_{-\infty}^{\infty} u(t - T_0)e^{j2\pi(f_0 + f_d)(t - T_0)}[u(t - T'_R)e^{j2\pi f_0(t - T'_R)}]^* \, dt$$

$$= \int_{-\infty}^{\infty} u(t - T_0)u^*(t - T'_R)e^{j2\pi(f_0 + f_d)(t - T_0)} e^{-j2\pi f_0(t - T'_R)} \, dt \tag{11.48}$$

It is customary to set $T_0 = 0$ and $f_0 = 0$, and to define $T_0 - T'_R = -T'_R = T_R$. The output of the matched filter is then

$$\chi(T_R, f_d) = \int_{-\infty}^{\infty} u(t)u^*(t + T_R)e^{j2\pi f_d t} \, dt \tag{11.49}$$

In this form a positive T_R indicates a target beyond the reference delay T_0, and a positive f_d indicates an incoming target.[13] The squared magnitude $|\chi(T_R, f_d)|^2$ is called the *ambiguity function* and its plot is the *ambiguity diagram.*

The ambiguity diagram has been used to assess the properties of the transmitted waveform as regards its target resolution, measurement accuracy, ambiguity, and response to clutter.

Properties of the ambiguity diagram. The function $|\chi(T_R, f_d)|^2$ has the following properties:

$$\text{Maximum value of } |\chi(T_R, f_d)|^2 = |\chi(0, 0)|^2 = (2E)^2 \tag{11.50}$$

$$|\chi(-T_R, -f_d)|^2 = |\chi(T_R, f_d)|^2 \tag{11.51}$$

$$|\chi(T_R, 0)|^2 = \left| \int u(t)u^*(t + T_R) \, dt \right|^2 \tag{11.52}$$

$$|\chi(0, f_d)|^2 = \left| \int u^2(t)e^{j2\pi f_d t} \, dt \right|^2 \tag{11.53}$$

$$\iint |\chi(T_R, f_d)|^2 \, dT_R \, df_d = (2E)^2 \tag{11.54}$$

The first equation given above, Eq. (11.50), states that the maximum value of the ambiguity function occurs at the origin and its value is $(2E)^2$, where E is the energy contained in the echo signal. Equation (11.51) is a symmetry relation. Equations (11.52) and (11.53) describe the behavior of the ambiguity function on the time-delay axis and the frequency axis, respectively. Along the T_R axis the function $\chi(T_R, f_d)$ is the autocorrelation function of the modulation $u(t)$, and along the f_d axis it is proportional to the spectrum of $u^2(t)$. Equation (11.54) states that the total volume under the ambiguity function is a constant equal to $(2E)^2$.

Ideal ambiguity diagram. If there were no theoretical restrictions, the ideal ambiguity diagram would consist of a single peak of infinitesimal thickness at the origin and be zero everywhere else, as shown in Fig. 11.7. The single spike eliminates any ambiguities, and its infinitesimal

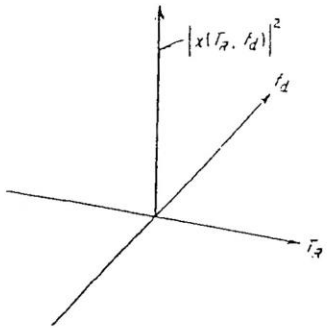

Figure 11.7 Ideal, but unattainable, ambiguity diagram.

thickness at the origin permits the frequency and the echo delay time to be determined simultaneously to as high a degree of accuracy as desired. It would also permit the resolution of two targets no matter how close together they were on the ambiguity diagram. Naturally, it is not surprising that such a desirable ambiguity diagram is not possible. The fundamental properties of the ambiguity function prohibit this type of idealized behavior. The two chief restrictions are that the maximum height of the $|\chi|^2$ function be $(2E)^2$ and that the volume under the surface be finite and equal $(2E)^2$. Therefore the peak at the origin is of fixed height and the function encloses a fixed volume. A reasonable approximation to the ideal ambiguity diagram might appear as in Fig. 11.8. This waveform does not result in ambiguities since there is only one peak, but the single peak might be too broad to satisfy the requirements of accuracy and resolution. The peak might be narrowed, but in order to conserve the volume under its surface, the function must be raised elsewhere. If the peak is made too narrow, the requirement for a constant volume might cause peaks to form at regions of the ambiguity diagram other than the origin and give rise to ambiguities. Thus the requirements for accuracy and ambiguity may not always be possible to satisfy simultaneously.

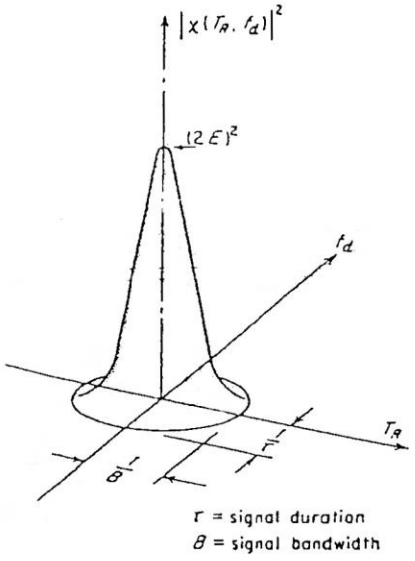

Figure 11.8 An approximation to the ideal ambiguity diagram, taking account the restrictions imposed by the requirement for a fixed value of $(2E)^2$ at the origin and a constant volume enclosed by the $|\chi|^2$ surface.

The ambiguity diagram in three dimensions may be likened to a box of sand. The total amount of sand in the box is fixed and corresponds to a fixed signal energy. No sand can be added, and none can be removed. The sand may be piled up at the center (origin) to as narrow a pile as one would like, but its height can be no greater than a fixed amount $(2E)^2$. If the sand in the center is in too narrow a pile, the sand which remains might find itself in one or more additional piles, perhaps as big as the one at the center.

The optimum waveform is one which has the desired ambiguity diagram for a given amount of "sand" (energy). The usual pulse radar or the usual CW radar, as we shall see, does not result in an ideal diagram. To produce an ambiguity diagram such as that shown in Fig. 11.8, the transmissions must be noiselike.

The synthesis of the waveform required to satisfy the requirements of accuracy, ambiguity, and resolution as determined by the ambiguity diagram is a difficult task. The usual design procedure is to compute the ambiguity diagram for the more common waveforms and to observe its behavior. Because of the limitations of synthesis, the ambiguity diagram has been more a measure of the suitability of a selected waveform than a means of finding the optimum waveform.

Single pulse of sine wave. The ambiguity diagram for a single rectangular pulse of sine wave is shown in Fig. 11.9. Contours for constant values of doppler frequency shift (velocity) are shown in Fig. 11.9*a*. The contour for zero velocity is triangular in shape and represents the autocorrelation function of a rectangular pulse such as would be predicted from Eq. (11.52). Contours for fixed values of time delay are shown in Fig. 11.9*b*. The center contour corresponding to $T_R = 0$ is the spectrum of a rectangular pulse [Eq. (11.53)]. The composite three-dimensional ambiguity surface is shown in Fig. 11.9*c*.

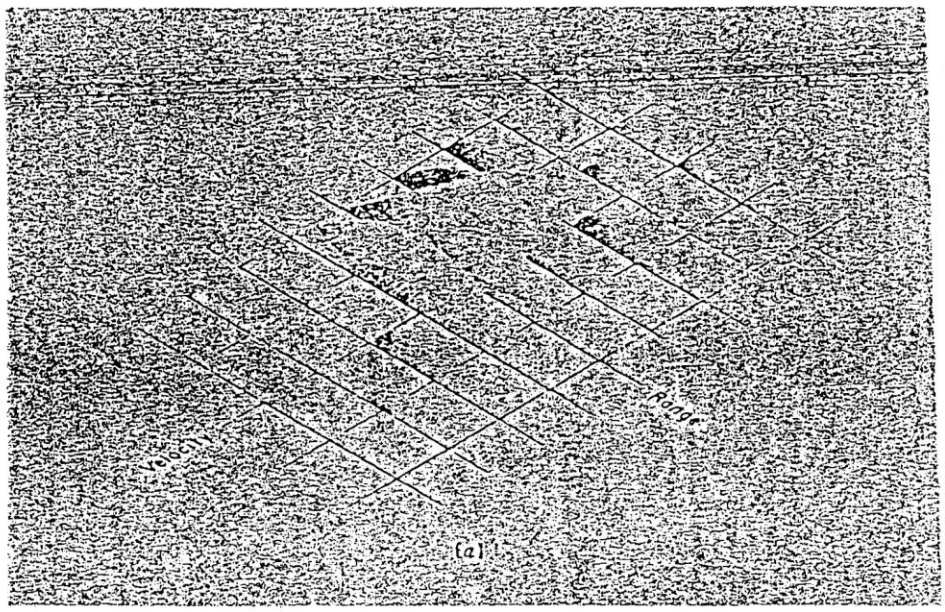

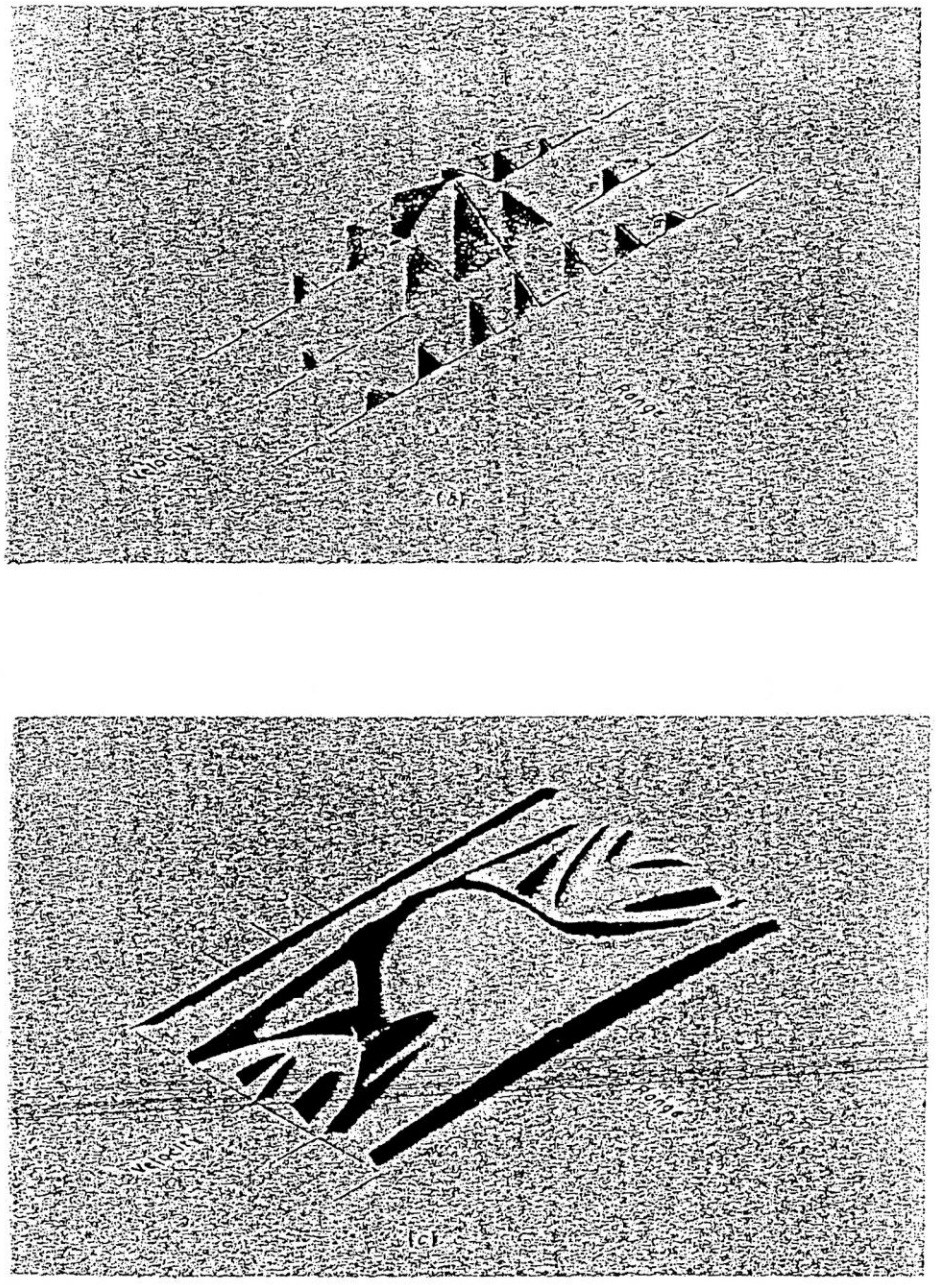

Figure 11.9 Three-dimensional plot of the ambiguity diagram for a single rectangular pulse. (*a*) Contours for constant dopppler frequency (velocity); (*b*) contours for constant time delay (range); (*c*) composite surface. (*Courtesy S. Applebaum and P. W. Howells, General Electric Co., Heavy Military Electronics Department, Syracuse, N.Y.*)

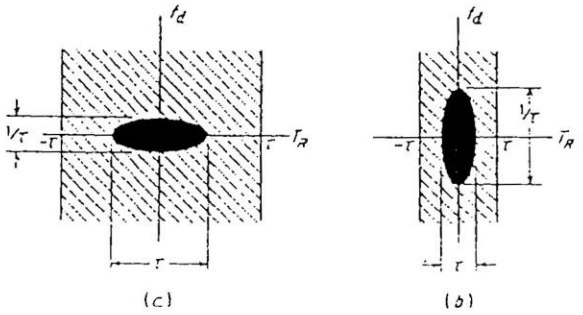

Figure 11.10 Two-dimensional ambiguity diagram for a single pulse of sine wave. (*a*) Long pulse; (*b*) short pulse.

It is usually inconvenient to draw a three-dimensional plot of the ambiguity diagram. For this reason a two-dimensional plot is often used to convey the salient features. Figure 11.10 is an example of the two-dimensional plot of the three-dimensional ambiguity diagram corresponding to the single pulse of Fig. 11.9*c*. Shading is used to give an indication of the regions in which $|\chi(T_R, f_d)|^2$ is large (completely shaded areas), regions where $|\chi|^2$ is small but not zero (lightly shaded areas), and regions where $|\chi|^2$ is zero (no shading). The plot for a single pulse shows a single elliptically shaped region in which $|\chi|^2$ is large. This is what would have been expected from our previous discussions since a single measurement does not result in ambiguity if the threshold is chosen properly. Range error is proportional to the pulse width τ, while doppler error is proportional to $1/\tau$. Shortening the pulse width improves the range accuracy, but at the expense of the doppler-velocity accuracy. Although the shape of the ellipse can be as thin or as broad as one likes in either axis, the opposite will be true for the other axis. The region in the vicinity of the origin cannot be made as small as we wish along both axes simultaneously without shifting some of the completely shaded region elsewhere in the diagram.

By letting τ become very large (essentially infinite), Fig. 11.10 may also be used to represent a CW radar. Similarly by letting τ be very small (infinitesimal), the diagram applies to an impulse radar.

Periodic pulse train. Consider a sinusoid modulated by a train of five pulses, each of width τ. The pulse-repetition period is T_p, and the duration of the pulse train is T_A (Fig. 11.11*a*). The ambiguity diagram is represented in Fig. 11.11*b*. With a single pulse the time-delay- and frequency-measurement accuracies depend on one another and are linked by the pulse width τ. The periodic train of pulses, however, does not suffer this limitation. The time-delay error is determined by the pulse width τ as before, but the frequency accuracy is determined by the total duration of the pulse train. Thus the time- and frequency-measurement accuracies may be made independent of one another.

For the privilege of independently controlling the time and frequency accuracy with a periodic waveform, additional peaks occur in the ambiguity diagram. These peaks cause ambiguities. The total volume represented by the shaded areas of the ambiguity diagram for the periodic waveform approximates the total volume of the ambiguity diagram of the single pulse, assuming that the energy of the two waveforms are the same. This follows from the relationship expressed by Eq. (11.54). In practice, the radar designer attempts to select the pulse-repetition period T_p so that all targets of interest occur only in the vicinity of the central peak, all other peaks being far removed from the region occupied by the targets. The periodic-pulse waveform is a good one from the point of view of accuracy if the radar application is

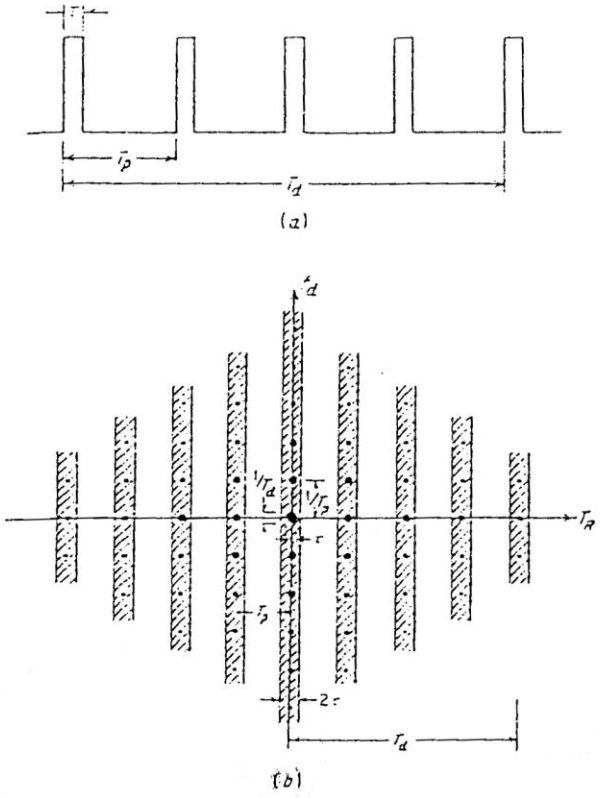

Figure 11.11 (*a*) Pulse train consisting of five pulses; (*b*) ambiguity diagram for (*a*).

such that it is possible to ignore or eliminate any ambiguities which arise. The fact that most practical radars employ this type of waveform attests to its usefulness far better than any theoretical analysis which might be presented here. It is encouraging, however, when theoretical considerations substantiate the qualitative, intuitive reasoning upon which most practical engineering decisions must usually be based, for lack of any better criterion.

Single frequency-modulated pulse. Ambiguities may be avoided with a single-pulse waveform rather than a periodic-pulse waveform. Although the accuracy of simultaneously measuring time and frequency with a simple pulse-modulated sinusoid was seen to be limited, it is possible to obtain simultaneous time and frequency measurements to as high a degree of accuracy as desired by transmitting a pulse long enough to satisfy the desired frequency accuracy and one with enough bandwidth to satisfy the time accuracy. In other words, the peak at the center of the ambiguity diagram may be narrowed by transmitting a pulse with a large bandwidth times pulse-width product (large $\beta\alpha$). One method of increasing the bandwidth of a pulse of duration T is to provide internal modulation. The ambiguity diagram for a frequency-modulated pulse is shown in Fig. 11.12. The waveform is a single pulse of sine wave whose frequency is decreased linearly from $f_0 + \Delta f/2$ to $f_0 - \Delta f/2$ over the duration of the pulse T, where f_0 is the carrier frequency and $\Delta f \approx B$ is the frequency excursion.

The ambiguity diagram is elliptical, as for the single pulse of unmodulated sine wave. However, the axis of the ellipse is tilted at an angle to both the time and frequency axes. This

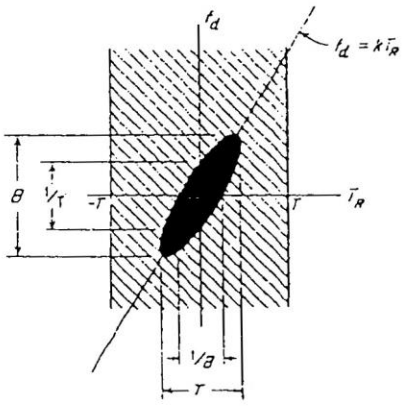

Figure 11.12 Ambiguity diagram for a single frequency-modulated pulse. (Also called the *chirp* pulse-compression waveform.)

particular waveform is not entirely satisfactory. The accuracy along either the time axis or the frequency axis can be made as good as desired. However, the accuracy along the ellipse major axis is relatively poor. This is a consequence of the fact that both the time delay (range) and the frequency (doppler) are both determined by measuring a frequency shift. Thus neither the range nor the velocity can be determined without knowledge of the other.

This limitation can be overcome by transmitting a second FM pulse whose slope on the ambiguity diagram is different from that of Fig. 11.12. The second modulation might be a linear frequency modulation which increases, rather than decreases, in frequency. This is analogous to the FM-CW radar of Chap. 3, in which the doppler frequency shift is extracted as well as the range. It will be recalled that the sawtooth frequency-modulated waveform of the FM-CW radar was capable of determining the range as long as there was no doppler frequency shift. By using a triangular waveform instead of the sawtooth waveform it was possible to measure both the range and the doppler frequency. The same technique can be used with the frequency-modulated pulse radar.

Classes of ambiguity diagrams. There are three general classes of ambiguity diagrams, Fig. 11.13. The knife edge, or ridge, is obtained with a single pulse of sine wave. Its orientation is along the time-delay axis for a long pulse, along the frequency axis for a short pulse, or it can be rotated to any direction in the τ_R, f_d plane by the application of linear frequency modulation. The bed of spikes in Fig. 11.13*b* is obtained with a periodic train of pulses. The internal structure of each of the major components, illustrated figuratively by the simple arrows, depends on the waveform of the individual pulses. The thumbtack ambiguity diagram, Fig. 11.13*c*, is obtained with noise or pseudonoise waveforms. The width of the spike at the center can be made narrow along the time axis and along the frequency axis by increasing the bandwidth and pulse duration, respectively. However, the plateau which surrounds the spike is more complex than illustrated in the simple sketch. With real waveforms, the sidelobes in the plateau region can be higher than might be desired. Furthermore, the extent of the platform increases as the spike is made narrower since the total volume of the ambiguity function must be a constant, as was given by Eq. (11.54). There can be many variations of these three classes, as illustrated in Ref. 11.

Transmitted waveform and the ambiguity function. The particular waveform transmitted by a radar is chosen to satisfy the requirements for (1) detection, (2) measurement accuracy, (3) resolution, (4) ambiguity, and (5) clutter rejection. The ambiguity function and its plot, the

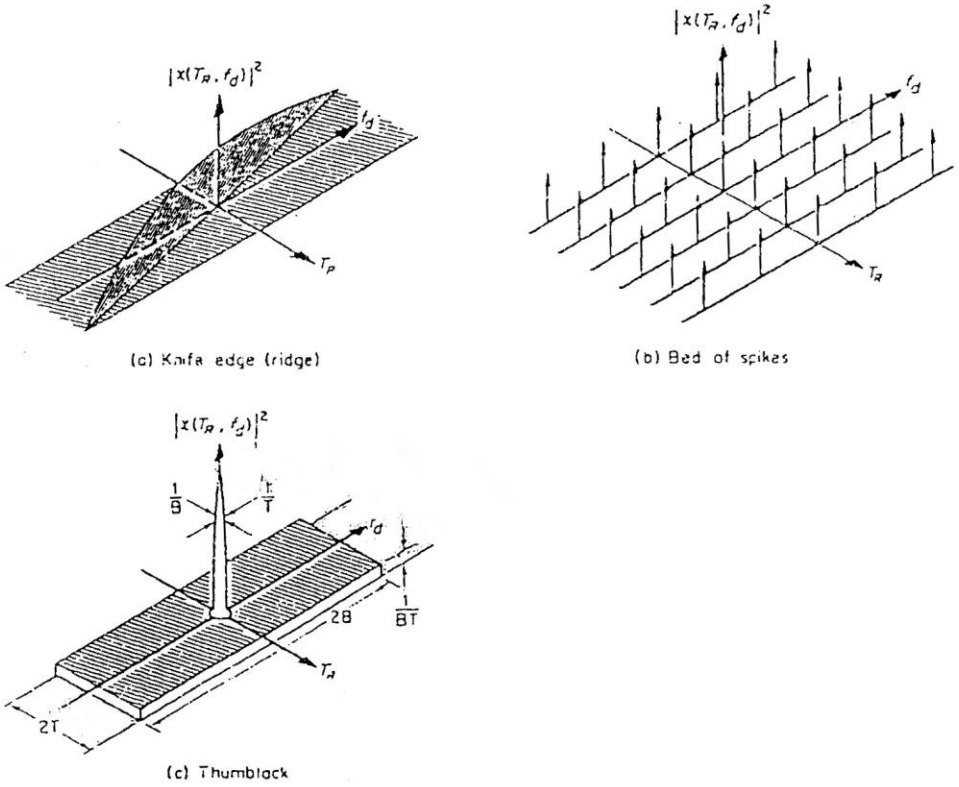

Figure 11.13 Classes of ambiguity diagrams: (*a*) knife edge, or ridge; (*b*) bed of spikes; (c) thumbtack. (*From G. W. Deley.*[12] *Courtesy McGraw-Hill Book Company.*)

ambiguity diagram, may be used to assess qualitatively how well a waveform can achieve these requirements. Each of these will be discussed briefly.

If the receiver is designed as a matched filter for the particular transmitted waveform, the probability of detection is independent of the shape of the waveform and depends only upon E/N_0, the ratio of the total energy E contained in the signal to the noise power per unit bandwidth. The requirements for *detection* do not place any demands on the *shape* of the transmitted waveform except (1) that it be possible to achieve with practical radar transmitters, and (2) that it is possible to construct the proper matched filter, or a reasonable approximation thereto. The maximum value of the ambiguity function occurs at $T_R = 0, f_d = 0$ and is equal to $(2E)^2$. Thus the value $|\chi(0, 0)|^2$ is an indication of the detection capabilities of the radar. Since the plot of the ambiguity function is often normalized so that $|\chi(0, 0)|^2 = 1$, the ambiguity diagram is seldom used to assess the detection capabilities of the waveform.

The *accuracy* with which the range and the velocity can be measured by a particular waveform depends on the width of the spike, centered at $|\chi(0, 0)|^2$, along the time and the frequency axes. The *resolution* is also related to the width of the central spike, but in order to resolve two closely spaced targets the central spike must be isolated. It cannot have any high peaks nearby that can mask another target close to the desired target. A waveform that yields good resolution will also yield good accuracy, but the reverse is not always so.

A continuous waveform (a single pulse) produces an ambiguity diagram with a single peak. A discontinuous waveform can result in peaks in the ambiguity diagram at other values of T_R, f_d. The pulse train (Fig. 11.11 or 11.13*b*) is an example. The presence of additional spikes can lead to *ambiguity* in the measurement of target parameters. An ambiguous measurement is one in which there is more than one choice available for the correct value of a parameter, but only one choice is appropriate. Thus the correct value is uncertain. The ambiguity diagram permits a visual indication of the ambiguities possible with a particular waveform. The ambiguity problem is characteristic of a single target, as is the detection and accuracy requirements of a waveform, whereas resolution is concerned with multiple targets.

The ambiguity diagram may be used to determine the ability of a waveform to reject clutter by superimposing on the T_R, f_d plane the regions where clutter is found. If the transmitted waveform is to have good clutter-rejection properties the ambiguity function should have little or no response in the regions of clutter.

The problem of synthesizing optimum waveforms based on a desired ambiguity diagram specified by operational requirements is a difficult one. The approach to selecting a waveform with a suitable ambiguity diagram is generally by trial and error rather than by synthesis.

In summary, this section has considered some of the factors which enter into the selection of the proper transmitted waveform. The problem of designing a waveform to achieve detection may be considered independently of the requirements of accuracy, ambiguity resolution, and clutter rejection. A waveform satisfies the requirements of detection if its energy is sufficiently large and if the receiver is designed in an optimum manner, such as a matched-filter receiver. Waveform shape is important only as it affects the practical design of the matched filter. The ability of a particular waveform to satisfy the requirements of accuracy, ambiguity, resolution, and clutter rejection may be qualitatively determined from an examination of the ambiguity diagram. In general, periodic waveforms may be designed to satisfy the requirements of accuracy and resolution provided the resulting ambiguities can be tolerated. A waveform consisting of a single pulse of sinusoid avoids the ambiguity problem, but the time delay and frequency cannot simultaneously be measured to as great an accuracy as might be desired. However, it is possible to determine simultaneously both the frequency and the time delay to any degree of accuracy with a transmitted waveform containing a large bandwidth pulse-width product (large $\beta\alpha$ product). The problem of synthesizing optimum waveforms from an ambiguity diagram specified by operational requirements is a difficult one and is often approached by trial and error

The name *ambiguity function* for $|\chi(T_R, f_d)|^2$ is somewhat misleading since this function describes more about the waveform than just its ambiguity properties. Woodward[5] coined the name to demonstrate that the total volume under this function is a constant equal to $(2E)^2$, independent of the shape of the transmitted waveform, [Eq. (11.54)]. Thus the total *area of ambiguity*, or uncertainty, is the same no matter how $|\chi(T_R, f_d)|^2$ is distributed over the T_R, f_d plane, as illustrated by the sandbox analogy mentioned earlier in this section. The reader is advised not to be distracted by trying to understand why this function is described by the ambiguous use of the term "ambiguity."

11.5 PULSE COMPRESSION

Pulse compression allows a radar to utilize a long pulse to achieve large radiated energy, but simultaneously to obtain the range resolution of a short pulse. It accomplishes this by employing frequency or phase modulation to widen the signal bandwidth. (Amplitude modulation is also possible, but is seldom used.) The received signal is processed in a matched filter that